24 GHz Radar Sensor integrates Patch Antenna and Frontend Module in single Multilayer LTCC Substrate

R. Kulke, C. Günner, S. Holzwarth, J. Kassner, A. Lauer, M. Rittweger, P. Uhlig, P. Weigand*

IMST GmbH, Carl-Friedrich-Gauss-Str. 2, D-47475 Kamp-Lintfort, Germany

*DuPont de Nemours GmbH, DuPont Str. 1, D-61352 Bad Homburg, Germany

+49-2842-981-214, +49-2842-981-499, kulke@imst.de

Abstract

The authors from IMST and DuPont have developed in joint project a RADAR demonstrator operating in the 24 GHz band. The sensor is designed to be used in vehicles as driver assistance system. FMCW method is utilized to measure distances up to 30 m or even more and velocity of obstacles around the car. Especially safety enhancement systems like collision warning and mitigation but also comfort features can be realized. Moreover, the sensor is capable to be integrated in manifold industrial applications where distance and velocity have to be determined with high precision. Another interesting field of application is the monitoring of buildings and real estates, because the module concept is qualified for the free 24 GHz ISM band, too. The main focus of the development is directed towards the reduction of costs in comparison with conventional sensors. Hybrid circuit technology using 5-layer LTCC tape 951 from DuPont Microcircuit Materials has been realized. The patch-antenna is printed on one side of the multilayer ceramic, while the RF frontend has been integrated on the opposite side. The HF part of the demonstrator is as small as 34 mm x 21 mm. Signal conversion and signal processing are executed on an external board with USB interface to a PC. A software with graphical user interface allows the setting of sensor and evaluation parameters.

Key words: Automotive Short Range Radar, 24 GHz ISM Band Sensor.

24 GHz Radar Frontend Module

The core of the Radar sensor is a 5-layer LTCC substrate utilizing DuPont's tape system 951 with gold and silver screen printed conductors, which enable a combination of soldered SMD components as well as gold wire-bonding of diode and transistor chip devices. The main advantages of this design are its compact size due to the high degree of integration, its low costs technology caused by utilizing standard screen printing technique and chip devices instead of expensive MMICs and its rugged design with laminated ceramic layers. FMCW (Frequency Modulated Continuous Wave) Radar method is utilized, which allows the accurate measurement of distances and relative velocity of objects. The operating band-width can be modified from 250 MHz (ISM-band) to about 2 GHz. This allows the use of the module as automotive short range radar (SRR, see Figure 10), where a high distance resolution and obstacle separation is required, as well as ISM-Band applications with coarse distance resolution. The antenna of the frontend module is integrated in the same LTCC stack on the opposite side of the HF-circuitry. A aperture coupling transition has been designed from the frontend side to a buried antenna feeding network. An array of 2 x 4 patches is responsible for the required beam-width. All these properties make the 24 GHz sensor module an interesting alternative to competitive solutions, e.g. [4]. Figure 1 illustrates the sensor frontend on DuPont's tape 951. Table 1 summarizes the specifications and the following sections will describe the designed components of the module: VCO, buffer amplifier, coupler, mixer, antenna and feeding network. Finally, measured and evaluated results will be presented.

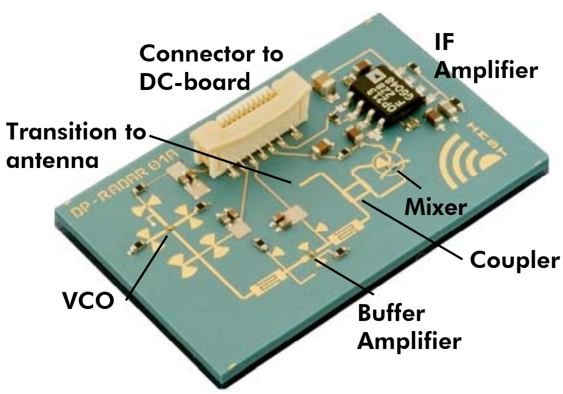

Figure 1: Frontend module on multilayer LTCC.

Parameters	Specifications
RADAR Method	FMCW
Center Frequency	24 GHz (f_{ISM} = 24.125 GHz)
Band-width	2 GHz (b_{ISM} = 250 MHz)
Resolution	± 1 cm
Obstacle Separation	± 10 cm
Distance	10 cm to 30 m
Output Power	< 10 dBm
Antenna Characteristic	± 15° Elevation ± 30° Azimuth

Table 1: Sensor Specifications

Components of the Frontend Module

The chain of circuit components starts with a voltage controlled oscillator (VCO) [2]. A single Varactor diode and FET transistor chip have been mounted on the LTCC substrate. Wire bonds connect the contact points on the chips with the screen printed gold conductors on the ceramic. The VCO is able to deliver 11 dBm output power up to 2 GHz band-width. To obtain a linear frequency modulated ramp for the FMCW method a band-width of 800 MHz to 1 GHz has been chosen for most of the following tests. It is also possible to operate the VCO in the ISM band at 24.125 GHz with 250 MHz band-width. Figure 1 shows the pushing behavior of the oscillator.

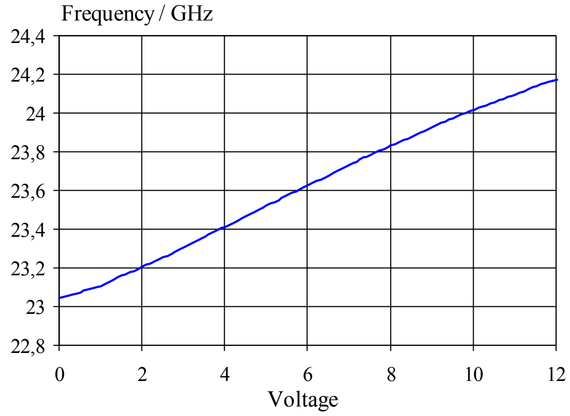

Figure 2: VCO frequency as a function of control voltage.

A buffer amplifier has been designed to separate the VCO from the output port. Two bandpass filters are used for RF and DC-decoupling. Most of the following experiments have been made with a demonstrator module without buffer amplifier.

A branch-line hybrid coupler is used to separate the transmit and receive signal. One port is connected with the transition to the antenna feeding network of the patch array, while the other ports are connected with the mixer. This component is a singly balanced mixer with a rat-race coupler and a device of series-pair diodes in one chip [1], which has been mounted in flip-chip configuration into the hybrid coupler. The conversion gain is plotted in Figure 3 with a LO power of 6 dBm.

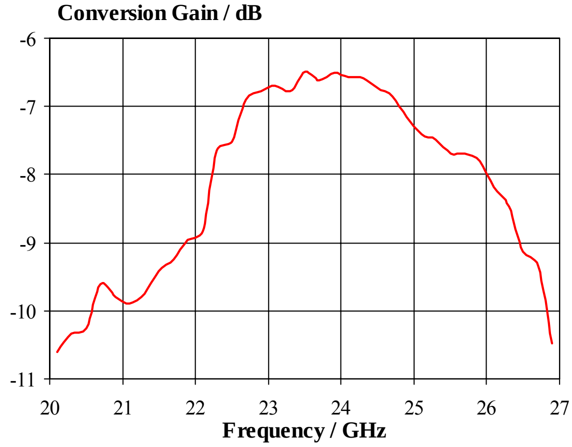

Figure 3: Conversion gain of mixer.

Planar Patch Antenna Array

A unique patch antenna has been developed for the Radar sensor [3], which is integrated on the same LTCC multilayer substrate on the opposite side of the HF frontend. Aperture coupling is utilized to achieve a reliable transition from the frontend circuit to the buried feeding network. The patch array is characterized by its broadband radiation performance, which has been achieved by a specific feeding geometry and configuration. The overall properties are: 10 dBi antenna gain, 10 dB bandwidth over 2.5 GHz, 3 dB beam-width: ±30° azimuth, ±15° elevation. Figure 4 illustrates the 2 x 4 patch array (yellow) with the buried feeding network (red) and the far-field characteristic of the antenna. 3D full wave simulations of the entire antenna have been carried out with the software tool Empire^{TM}, which is based upon the Finite Differences Time Domain method.

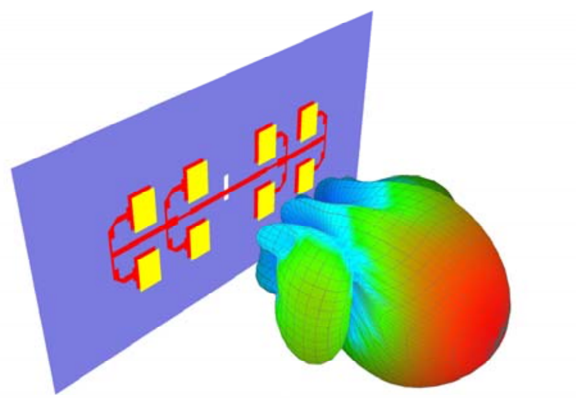

Figure 4: Far-Field pattern of 2 x 4 patch array.

Demonstrator Unit

The whole demonstrator unit consists of the LTCC Radar frontend with antenna, a µ-processor and power supply board with USB interface and a software with graphical user interface. The demonstrator is shown on a photo in Figure 5. The processor unit in the silver box combines a 32 MHz micro controller for ramp generation and data processing. For base-band operations a 10 bit D/A converter and a 4 channel 16 bit A/D converter is utilized. The USB interface delivers the DC power supply (5V, 500mA max.) for the entire demonstrator unit. The frontend module requires about 4V at 25mA. The current IF (Intermediate Frequency) signal level is about: $U_{IF} \approx 100\ \mu V$, $f_{IF} < 3$ kHz.

Figure 5: Sensor demonstrator module.

A specific software with graphical user interface has been developed. The software tool allows several interface and hardware settings, initializes the ramp for the FMCW Radar method, sets a number of parameters for data processing and evaluation, performs the DFT (Digital Fourier Transformation) and plots the time and frequency signals.

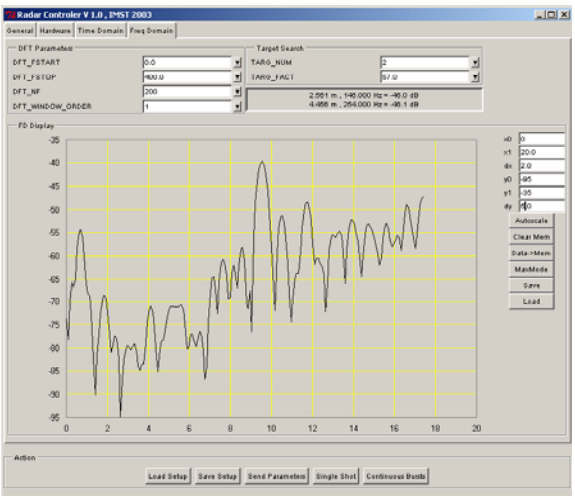

Figure 6: Frequency domain settings and plot of evaluation software with graphical user interface.

Figure 6 shows the frequency domain window of the software tool with typical parameter settings for the DFT and a plot of the transformed signal. The peaks in the curve represent reflections of objects in the environment around the sensor. The distance to the objects can be read from the X-axis of the diagram. Tests have been performed with the hardware and software to demonstrate its capabilities. Some experiments are described in the following sections with a frequency band-width of 800 MHz. More tests will be carried out to improve the demonstrator. This does also include modifications of the frontend module to achieve an enhancement of the sensor's performance.

An outdoor experiment has been made on the site of IMST. The sensor has been adjusted to a row of parking cars in a distance of roughly 40 m. In a second test the sensor has been adjusted to the sky to obtain a reference signal. The results of both measurements are plotted in Figure 7. A peak at 38.9 m in the read curve differs from the sky signal. An other significant peak appears at about 5 m in both plots. It turned out that this reflection comes from a wall of the building on the side of the sensor. This experiment makes obvious, that even strong objects like cars can be measured beyond a distance of 30 m. However, a higher averaging parameter than for low distance objects has to be selected.

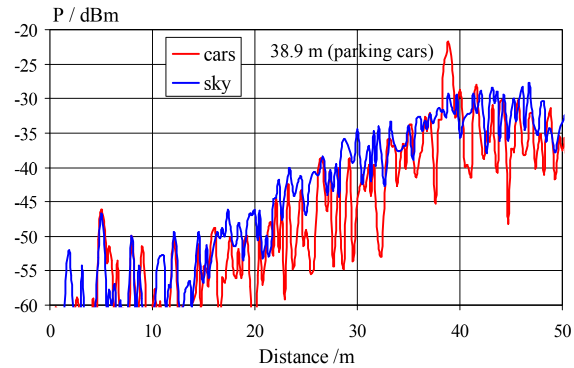

Figure 7: Measured distances to parking cars.

The next tests have been carried out with a frequency band-width of 800 MHz, because the ramp did show an optimal linearity in this range. The first test to determine the error of the sensor has been made to detect and measure cars on the street in distances between 2 and 16 m. The real and measured distance, the deviation and error are listed in Table 2. The corresponding curves are plotted in Figure 8. It becomes obvious, that the error is higher in close distance to the sensor. Good results could be achieved in a medium range, while the error increases again for farther objects.

Distance	2.0	5.6	9.7	13.7	15.1
Measured	2.3	5.5	9.6	13.3	14.5
Deviation	+0.3	-0.1	-0.1	-0.4	-0.6
Error	+15 %	-1.8 %	-1 %	-2.9 %	-4.1 %

Table 2: Measured distances and deviation in meters

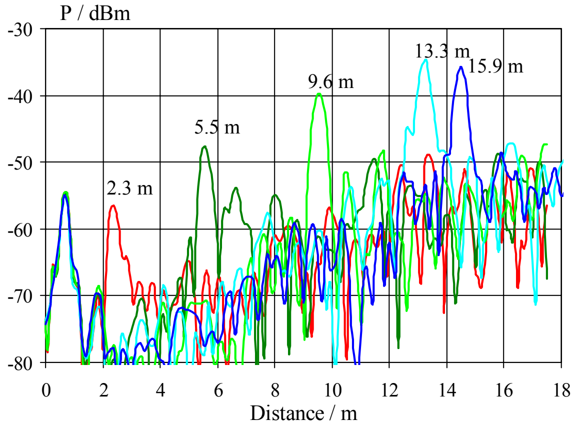

Figure 8: Measured distances to cars on a street (b = 800 MHz).

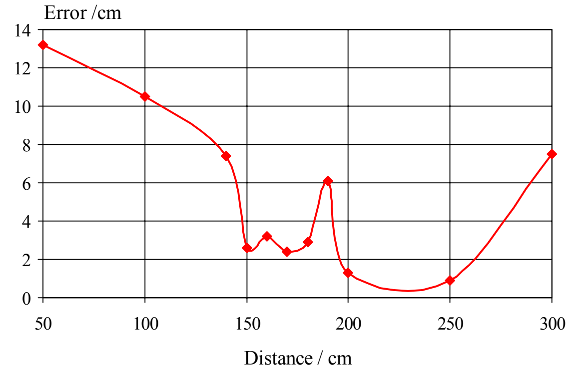

Figure 9: Error measurement (b = 800 MHz).

It turned out, that distance calibration is accurate in a specific range in front of the sensor. A calibration for long distances is not suitable for short distances and vice versa. That's why the calibration has been renewed for shorter distances around 2 m, which was worse in the preceding test. Figure 9 shows a curve with new measurements, where the error is plotted in a range from 0.5 to 3 m. Now the error is below 3% for 1.5 to 3.4 m. Again, a bandwidth of 800 MHz has been chosen to get best linearity of the VCO. A final evaluation software would include suitable calibration and parameter settings for different ranges.

Outlook

IMST is currently improving the frontend module. Especially the voltage controlled oscillator is still under investigation and will be redesigned to enhance the linearity and the bandwidth. A sensor with monolithic integrated VCO is in preparation to compare hybrid and MMIC solution. It is expected, that the final sensor for automotive application will have a total size of (60 x 45 x 20)mm^3 including antenna, Radar frontend, µ-processor board, interface and housing.

Up to now only distance measurement has been implemented and tested into the demonstration sensor. In further development steps velocity measurement will be added to the evaluation software followed by specific speed tests. Two methods are possible to determine the relative velocity of objects: by evaluating the Doppler shift at a single frequency or by evaluating the rising and falling slope of the frequency modulated ramp.

The Radar demonstrator is a first step towards a product. IMST and DuPont offer further development taking individual specifications into account. Parameters like costs, dimensions or functionality can be adapted to specific requirements.

References

[1] Stephen A. Maas: "Microwave Mixers", Second Edition, Artech House, 1993

[2] Stephen A. Maas: "Non-linear Microwave Circuits", IEEE-Press, 1997

[3] S. Holzwarth, R. Kulke, J. Kassner: "Integrated stacked patch antenna array on LTCC material operating at 24 GHz", IEEE AP-S International Symposium on Antennas and Propagation, Monterey, California, June 20-26, 2004.

[4] J. Wenger: "Microwave Components for Commercial Radar Applications", EEEfCOM proceedings, Ulm, Germany, June 2002

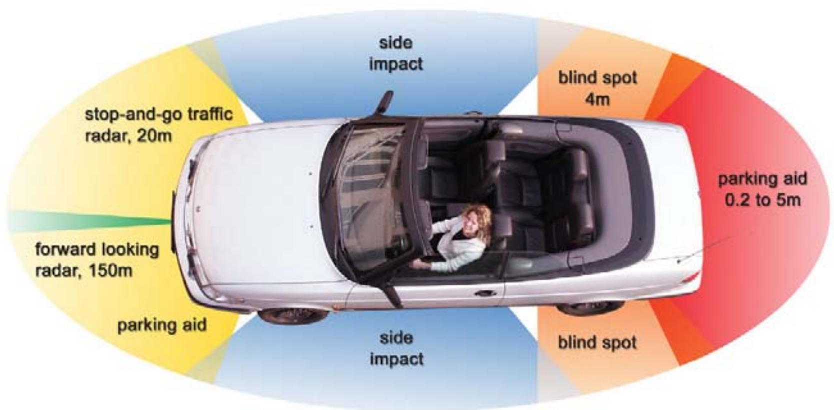

Figure 10: Applications for automotive sensors.